Songklanakarin J. Sci. Technol.
32 (4), 391-402, Jul. - Aug. 2010

Songklanakarin Journal of Science and Technology
http://www.sjst.psu.ac.th

Original Article

Effect of aggregate type, casting, thickness and curing condition on restrained strain of mass concrete

Pongsak Choktaweekarn* and Somnuk Tangtermsirikul

Construction and Maintenance Technology Research Center, Sirindhorn International Institute of Technology, Thammasat University, Pathum Thani, 12120 Thailand.

Received 5 January 2009; Accepted 5 July 2010

Abstract

In this paper, a three-dimensional finite element analysis is used for computing temperature and restrained strain in mass concrete. The model takes into account time, material properties, and mix proportion dependent behavior of concrete. The hydration heat and thermal properties used in the finite element analysis are obtained from our previously proposed adiabatic temperature rise model and are used as the input in the analysis. The analysis was done by varying size of mass concrete (especially thickness) and the casting method in order to explain their effect on temperature and restrained strain in mass concrete. The casting methods used in the analysis are continuous and discontinuous casting. The discontinuous casting consists of layer casting and block casting. Different types of aggregate were used in the analysis for studying the effect of thermal properties of aggregate on temperature and restrained strain in mass concrete. Different conditions of curing (insulation and normal curing) were also studied and compared. It was found from the analytical results that the maximum temperature increases with the increase of the thickness of structure. The use of layer casting is more effective for thermal cracking control of mass concrete. The insulation curing method is preferable for mass concrete. Aggregate with low coefficient of thermal expansion is beneficial to reduce the restrained strain.

Keywords: finite element analysis, semi-adiabatic temperature, restrained strain, mass concrete, thermal cracking

1. Introduction

Mass concrete is defined for large dimension construction such as dams, and mat foundations. In massive concrete structures, the temperature rise due to heat of hydration causes the temperature gradients which can induce cracks especially at early age. In some construction projects, thermal insulating blankets were used to minimize the interior and exterior concrete temperature gradient (Whittier *et al.*, 2004). Generally, for crack control, maximum temperature difference within the concrete mass should not exceed 20°C (Neville, 1995), but with limestone aggregate, the difference can be allowed up to 31°C (Portland Cement Association, 2003). The prediction of temperature gradient of mass concrete is essentially useful for crack control analysis and design. Several techniques have been reported in the literature for evaluation of the thermal stress and specifying construction technique. For example, the U.S. Army Corps of Engineers, in Engineering and Technical Letter (1997) and ACI (2005) provide design guides for thermal analysis of mass concrete. However, those design guides are complicate for manual calculation and cannot be used for various types of cementitious materials or complicate methods of construction. Many researchers have developed models to simulate temperature of mass concrete (Isgor and Razaqpur, 2004; Kwak *et al.*, 2006; Sarker *et al.*, 1999; Maekawa *et al.*, 1999; Wang and Dilger, 1994; Park *et al.*, 2008; Faria *et al.*, 2006; Saengsoy and Tangtermsirikul, 2003). Some of them did not include the effect of fly ash (Isgor and Razaqpur, 2004; Park *et al.*, 2008). In this study, the adiabatic temperature rise model which was devel-

* Corresponding author.
Email address: pongsak@siit.tu.ac.th

oped by Saengsoy and Tangtermsirikul (2003) to predict heat generated from the hydration and pozzolanic reaction and adiabatic temperature rise of mass concrete with fly ash is adopted. Details of the model are briefly mentioned in section 2. Verifications of the model showed that the proposed model was satisfactory for predicting the adiabatic temperature of various test results. Heat of hydration and pozzolanic reactions which was obtained from the adiabatic temperature rise model was used as the input for a FEM program, MARC, by Choktaweekarn and Tangtermsirikul (2007) to analyze the semi-adiabatic temperature rise of concrete. Details of the model were mentioned in Choktaweekarn and Tangtermsirikul (2007). The verifications showed that the model were satisfactory for predicting temperature of the test results in laboratory and measured results in some real mass concrete footings. In this paper, FEM program was used to calculate not only the semi-adiabatic temperature but also restrained strain. The analytical results of the proposed model were verified with the test results obtained from the real mass concrete footing. An example of the verification for a real mass concrete footing is shown in section 3. Tensile strain capacity (TSC) of concrete is used as the criterion of failure to evaluate thermal cracking in mass concrete (Lu *et al.*, 2001; Tongaroonsri and Tangtermsirikul, 2008). TSC of concrete used in this study was obtained from Tongaroonsri and Tangtermsirikul (2008) and test results conducted by Lu *et al.* (2001).

In the case of massive concrete with very large size, casting usually cannot be finished at one time. Technique of discontinuous casting typically layer casting or block casting was used in order to minimize temperature gradient of mass concrete. The selection of proper dimension and numbers of concrete blocks or layers in order to prevent thermal cracking is one of the important steps for mass concrete construction. The use of different type of aggregate has an effect on thermal properties of concrete which influences semi-adiabatic temperature and thermal stress. Curing method and curing period are also important to prevent thermal cracking during the construction process. Many massive structures crack because of the application of unsuitable curing method and curing period. The objectives of this study are to explain and propose a method to compute the temperature and restrained strain in mass concrete by taking into account the footing dimension, casting method, aggregate type, curing condition and curing period in order to prevent thermal cracking.

2. Method of Analysis

Heat of hydration and pozzolanic reaction which were obtained from adiabatic temperature rise model were used as the input for a FEM program, MARC. Thermal properties; which are specific heat, thermal conductivity and coefficient of thermal expansion (CTE) are obtained from Choktaweekarn *et al.* (2009a), Choktaweekarn *et al.* (2009b) and Choktaweekarn and Tangtermsirikul, (2006), respectively. FEM program was used to analyze the semi-adiabatic temperature rise of concrete. For the proposed model, three dimensional eight-node brick was used in the analysis. The considered time interval is divided into several increments, each increment equals to one hour. The couple thermo-mechanical problem was used in the analysis in which thermal analysis is solved first. The temperature obtained from the thermal analysis is used as the input for the computation of the restrained strain. The details are elaborated below.

2.1 Thermal analysis

By the use of the common thermal analysis which was mentioned by many researchers (Isgor and Razaqpur, 2004; Kwak *et al.*, 2006; Sarker *et al.*, 1999; Maekawa *et al.*, 1999; Wang and Dilger, 1994; Park *et al.*, 2008; Faria *et al.*, 2006) with the heat of hydration and pozzolanic reaction and thermal properties models obtained from Saengsoy and Tangtermsirikul (2003), Choktaweekarn *et al.* (2009a), Choktaweekarn *et al.* (2009b), Choktaweekarn and Tangtermsirikul (2006) and Choktaweekarn and Tangtermsirikul, (2009), the semi-adiabatic temperature distribution in the concrete mass can be analyzed.

The governing equation of heat transfer for temperature prediction of mass concrete with consideration of heat of hydration is shown in Eq. (1).

$$\rho c \frac{\partial T}{\partial t} = q_{hy} + \frac{\partial}{\partial x}\left(k_x \frac{\partial T}{\partial x}\right) + \frac{\partial}{\partial y}\left(k_y \frac{\partial T}{\partial y}\right) + \frac{\partial}{\partial z}\left(k_z \frac{\partial T}{\partial z}\right) \quad (1)$$

where: k_x, k_y, k_z are the thermal conductivity of concrete in x, y and z direction, respecitvely (kcal/m hr °C). r is concrete density (kg/m^3), c is specific heat of concrete (kcal/ kg °C), q_{hy} is the rate of internal heat generated by hydration and pozzolanic reaction per unit volume (kcal/m^3 hr). t is age of concrete (hr.). T is temperature of concrete (°C).

The total heat generation of concrete was computed from the summation of the heat liberated due to the reaction of each cement compounds including the formation of ettringite and monosulphate and the reaction of fly ash as

$$Q(t) = Q_{C_3S}(t) + Q_{C_2S}(t) + Q_{C_3A}(t) + Q_{C_4AF}(t) + Q_{C_3AET}(t) + Q_{C_4AFET}(t) + Q_{FA}(t) \quad (2)$$

where Q(t) is the total heat generation of concrete at the considered age (kcal/kg of concrete). $Q_{C_3S}(t)$, $Q_{C_2S}(t)$, $Q_{C_3A}(t)$, $Q_{C_4AF}(t)$, and $Q_{FA}(t)$ are the cumulative heat generation of C_3S, C_2S, C_3A, C_4AF, and fly ash, respectively, at the considered age (kcal/kg of concrete). $Q_{C_3AET}(t)$ and $Q_{C_4AFET}(t)$ are cumulative heat generation of the ettringite and monosulphate formation by C_3A, and C_4AF reacting with gypsum, respectively, at the considered age (kcal/kg of concrete).

Some details for calculation of heat generation are briefly mentioned below. More details can be found in Saengsoy and Tangtermsirikul (2003). The cumulative heat generation of each cement compound was considered to be

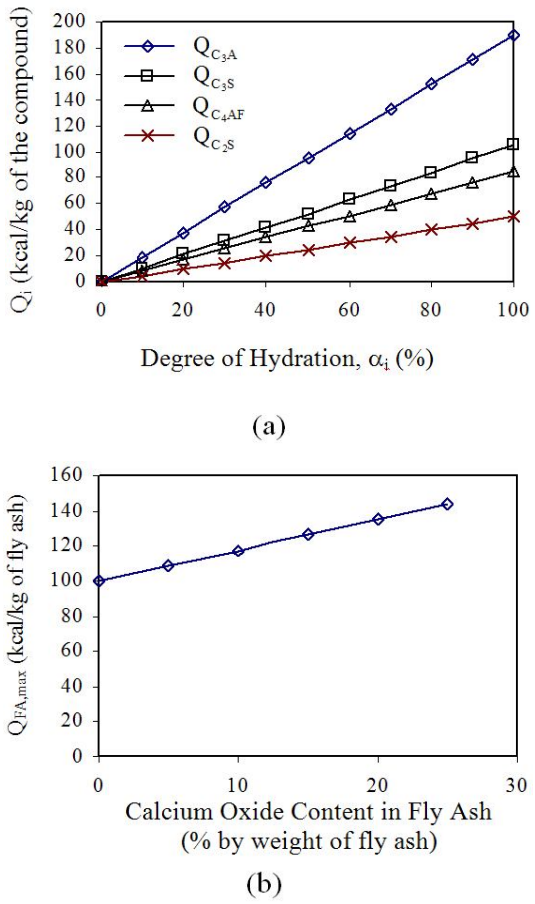

Figure 1. Cumulative heat generation of (a) C_3S, C_2S, C_3A, and C_4AF at different degree of hydration, (b) fly ash at the maximum pozzolanic reaction with various calcium oxide content in fly ash

linearly related to its degree of reaction and its content in the concrete as shown in Eq. (3). Figure 1a shows the cumulative heat generation of C_3S, C_2S, C_3A, and C_4AF at different degree of hydration. The cumulative heat generation of fly ash was computed based on the degree of pozzolanic reaction and fly ash content in concrete as shown in Eq. (4). The cumulative heat generation of fly ash at its maximum pozzolanic reaction degree ($Q_{FA,max}$) is assumed to be the function of calcium oxide content in fly ash as can be seen in Figure 1b.

$$Q_i(t) = \frac{\alpha_i(t)}{100} \cdot Q_{i,max} \cdot w_i \quad (3)$$

$$Q_{FA}(t) = \frac{\alpha_{poz}(t)}{100} \cdot Q_{FA,max} \cdot w_{fa} \quad (4)$$

where $Q_i(t)$ is the cumulative heat generation of each cement compound i and $Q_{FA}(t)$ is the cumulative heat generation of fly ash at the considered age (kcal/kg of concrete). $\alpha_i(t)$ and $\alpha_{poz}(t)$ are the degree of hydration of each cement compound i and the degree of pozzolanic reaction at the considered age (%). $Q_{i,max}(t)$ and $Q_{FA,max}(t)$ are the cumulative heat generation of each cement compound i and fly ash at their complete reaction at the considered age (kcal/kg). w_i and w_{fa} are the effective weight ratio of each cement compound i and fly ash available to generate heat in 1 m^3 of concrete to the unit weight of concrete.

Specific heat and thermal conductivity used in the analysis were obtained from Choktaweekarn *et al.* (2009a) and Choktaweekarn *et al.* (2009b) as shown in Eqs (5) and (6).

$$c(t) = w_g c_g + w_s c_s + w_{ra} c_{ra} + w_{fw}(t) c_w + w_{uc}(t) c_c + w_{ufa}(t) c_{fa} + w_{hp}(t) c_{hp} \quad (5)$$

$$k(t) = n_g k_g + n_s k_s + n_{fw}(t) k_w + n_{uc}(t) k_c + n_{ufa}(t) k_{fa} + n_{ra} k_{ra} + n_{hp}(t) k_{hp} \quad (6)$$

where c(t) is the specific heat of concrete at the considered age (kcal/kg °C). w_{ra}, w_g, and w_s are the weight ratio of air, coarse aggregate, and sand per unit weight of concrete, respectively (kg / kg of concrete). $w_{fw}(t)$, $w_{uc}(t)$, $w_{ufa}(t)$, and $w_{hp}(t)$ are the weight ratio of free water, unhydrated cement, non-reacted fly ash, and the hydration and pozzolanic products, respectively, at the considered age (kg / kg of concrete). c_g, c_s, c_w, c_c, c_{fa}, c_{ra} and c_{hp} are the values of specific heat of coarse aggregate, sand, water, cement, fly ash, air and the hydration and pozzolanic products, respectively (kcal/kg °C). k(t) is thermal conductivity of concrete at any age (kcal/m.hr °C), k_g, k_s, k_w, k_c, k_{fa}, k_{ra}, k_{hp} are thermal conductivity of coarse aggregate, sand, water, cement, fly ash, air and the hydrated product, respectively (kcal/m.hr °C). $n_{fw}(t)$, $n_{uc}(t)$, $n_{ufa}(t)$, $n_{hp}(t)$ are volumetric ratio of free water, non-reacted cement, unhydrated fly ash and the hydrated product, respectively, at the time considered (m^3/m^3 of concrete). n_g, n_s, n_{ra} are volumetric ratio of coarse aggregate, sand and air, respectively (m^3/m^3 of concrete).

Specific heat and thermal conductivity of each ingredient of concrete are shown in Table 1. Equations for predicting these two thermal properties of concrete were proposed as time, material and mix proportion dependent functions. The equations were verified with various experimental results and the verification results were satisfactory. The details of the model are not mentioned here but are elsewhere (Choktaweekarn *et al.*, 2009a; Choktaweekarn *et al.*, 2009b).

The heat transfer inside the concrete mass is governed by Eq. (1), however, the condition at the concrete surface is different. The conduction process plays an important role in transferring heat within the interior elements. However, for exterior elements, the conduction play a dominant role in transferring heat within the concrete while the presence of wind and solar radiation affect the temperature profile significantly and must be considered. Convective heat transfer refers to the heat that transfers between a solid and a moving fluid or gas for a temperature gradient between both materials. In this case, the convective heat transfer is involved in transferring heat between surface of mass concrete and

Table 1. Thermal properties of the ingredients in concrete

Thermal Coefficients	Limestone	Quartz Sand	Air	Water	Cement	Fly Ash	Hydrated Product
k (kcal/ m hr °C)	2.2	3.0	0.022	0.51	1.33	0.65	1.0
c (kcal/kg °C)	0.2	0.19	0.24	1.0	0.18	0.17	0.1
CTE (micron/°C)	4.5	10.4	-	-	14.4	6.45	20

Remark: k, c, CTE are thermal conductivity, specific heat and thermal expansion coefficient, respectively

environment (between concrete and air). The amount of heat transfer per unit surface through convection at the surface of concrete can be calculated according to Newton's cooling law. The convection heat transfer coefficient, *h*, is dependent on the type of media, gas or liquid, the flow properties such as velocity, viscosity and other flow and temperature dependent properties. For simplicity, the radiation is usually accounted together with the convection, through a single convection-radiation coefficient (Faria *et al.*, 2006). The convective heat transfer at concrete surface can be expressed as

$$q = h(T_s - T_a) \tag{7}$$

where q is the convective heat flux per unit area, h is the combined convection-radiation heat transfer coefficients (kcal/m^2 hr ^{o}C), T_s and T_a are the surface and air temperature.

In the real mass concrete footing, heat loss to surrounding air is also processed by convection. Normally, the side and bottom surfaces of a footing are covered by subsoil and heat dissipates from concrete to the surrounding soil by conduction process. However, the problem can be simplified by the assumption that the amount of heat loss to the surrounding subsoil is assumed to be done by the convection process. This kind of assumption and boundary condition were used in previous study of other researchers (Faria *et al.*, 2006).

In order to simulate the actual condition as that occurred in a real concrete footing, some parameters used in the analysis were assumed to be under the same condition as that occurred in a real concrete footing of a construction project in Bangkok, Thailand. In the analysis, *h* at the top surface are equal to 4 and 10.6 kcal/m^2 hr °C for insulation (IC) and normal curing (NC), respectively. *h* at the bottom and side surfaces is assumed to be equal to 2.5 kcal/m^2 hr °C . The average annual temperature in Bangkok which is equal to 28.7°C (Jindawanik *et al.*, 2000) is used as the atmospheric boundary condition. The initial condition of concrete is the initial temperature of concrete which is assumed to be 30°C. The model was verified with the test results conducted in the lab and the measured results of real footings. The verifications were shown in Choktaweekarn and Tangtermsirikul (2007). Verifications with the measured results of some real footings are shown in Figures 2a to 2c (Footing no. F1 to F3, respectively). Mix proportions of the

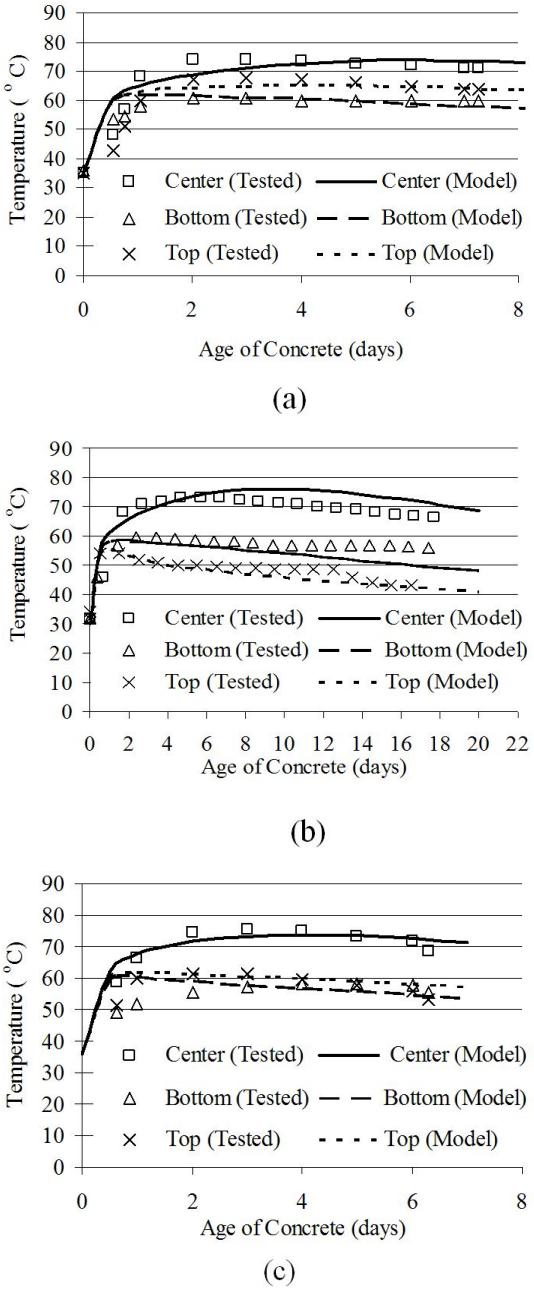

Figure 2. Comparison between test and predicted temperature at top, center and bottom of footing (a) Footing no. F1 (b) Footing no. F2, (c) Footing no. F3.

Table 2. Details of mix proportions of footings

Footing No.	Dimension(m.)	Ingredients (kg/m^3)				
		Cement	Fly Ash	Water	Sand	Coarse Aggregate
F1	16.4x21.15x3	196	196	166	730	1130
F2	38.4x8.4x4.75	225	125	170	855	1080
F3	13.2x24.9x2.5	210	190	160	810	1010
F4	14 x 63 x 1.4	242	198	185	780	1000

footings are shown in Table 2. The verifications show that the model is satisfactory for predicting temperature of the measured footings.

2.2 Restrained strain analysis

In each time step, the temperature at each position in mass concrete obtained from heat transfer analysis is used as the input for the restrained strain analysis. The internal deformation and stress in each element are related by Hooke's law as shown in Eq. (8).

The restrained strain is defined in Eq. (9). In case of absence of external loading, the stresses that cause cracking of early age concrete are induced by the restraint of deformations. Thermal strain of concrete element subject to temperature change can be calculated from Eq. (10). The effect of creep and shrinkage strain are not included in the analysis, then the difference between total strain and thermal strain becomes the restrained strain in concrete and the stress-strain relation in Eq (8) is transformed to be Eq. (11).

$$\{\Delta\sigma(t)\} = E(t)[\overline{D}]\{\Delta\varepsilon_{res}(t)\} \quad (8)$$

$$\{\Delta\varepsilon_{res}(t)\} = \{\Delta\varepsilon_{T}(t)\} - (\{\Delta\varepsilon_{cr}(t)\} + \{\Delta\varepsilon_{sh}(t)\} + \{\Delta\varepsilon_{th}(t)\}) \quad (9)$$

$$\Delta\varepsilon_{th}(t) = CTE\,(t)\Delta T(t) \quad (10)$$

$$\{\Delta\sigma(t)\} = E(t)[\overline{D}](\{\Delta\varepsilon_{T}(t)\} - \{\Delta\varepsilon_{th}(t)\}) \quad (11)$$

where $\Delta\sigma(t)$ is the change of stress at the considered age (MPa), $\Delta\varepsilon_{T}(t)$, $\Delta\varepsilon_{res}(t)$, $\Delta\varepsilon_{cr}(t)$, $\Delta\varepsilon_{sh}(t)$ and $\Delta\varepsilon_{th}(t)$ are the changes of total strain, restrained strain, creep strain, shrinkage strain and thermal strain at the considered age, respectively (micron). CTE(t) is the coefficient of thermal expansion coefficient (micron/°C) and $\Delta T(t)$ is the temperature change at the considered age (°C). $E(t)$ is the modulus of elasticity at the considered age (MPa). $[\overline{D}]$ is the material properties matrix and t is the considered age.

CTE of concrete is obtained from Choktaweekarn and Tangtermsirikul (2006) as shown in Eq. (12).

$$\mathrm{CTE}(t) = \frac{n_p \mathrm{CTE}_p(t) E_p(t) + n_s \mathrm{CTE}_s E_s + n_g \mathrm{CTE}_g E_g}{n_p E_p(t) + n_s E_s + n_g E_g} \quad (12)$$

where *CTE*(t) is the coefficient of thermal expansion of mortar or concrete at the considered age (micron/°C). $CTE_p(t)$, CTE_s, and CTE_g are the values of coefficient of thermal expansion of paste, fine aggregate and coarse aggregate, respectively (micron/°C). n_p, n_s, and n_g are the volumetric ratios of paste, fine aggregate, and coarse aggregate, respectively (m^3/m^3 of concrete). $E_p(t)$, E_s, and E_g are the modulus of elasticity of paste, fine aggregate, and coarse aggregate, respectively, (MPa), t is the considered age (day).

CTE of paste can be obtained from Choktaweekarn and Tangtermsirikul (2009) as shown in Eq. (13).

$$\mathrm{CTE}_p(t) = a \times n_{p,uc}(t)\mathrm{CTE}_c + b \times n_{p,ufa}(t)\mathrm{CTE}_{fa} + c \times n_{p,hp}(t)\mathrm{CTE}_{hp} \quad (13)$$

where $CTE_p(t)$ is the coefficient of thermal expansion of paste at the considered age (micron/°C). CTE_c, CTE_{fa}, and CTE_{hp} are the values of the coefficient of thermal expansion of cement, fly ash, and the hydration and pozzolanic reaction products, respectively (micron/°C). $n_{p,uc}(t)$, $n_{p,ufa}(t)$, and $n_{p,hp}(t)$ are the volumetric ratios, at the considered age, of unhydrated cement, non-reacted fly ash, and the hydration and pozzolanic reaction products, respectively (m^3/m^3 of paste). The constants a, b and c are derived to be equal to 0.284, 1.230 and 1.499, respectively.

3. Examples of analytical results and verification of the model to predict thermal cracking of mass concrete

The model was verified with a real concrete footing of a construction project in Bangkok, Thailand. Footing number F4 in Table 2 is used for this verification. Figure 3a shows a thermal crack at one side of the footing. The size of the footing was 14 x 63 x 1.4 m. The footing was cured by insulation curing for 4.6 days. Cracks were found right after the removal of the insulation materials. This means that cracks might occur since early age before the removal of the insulation material.

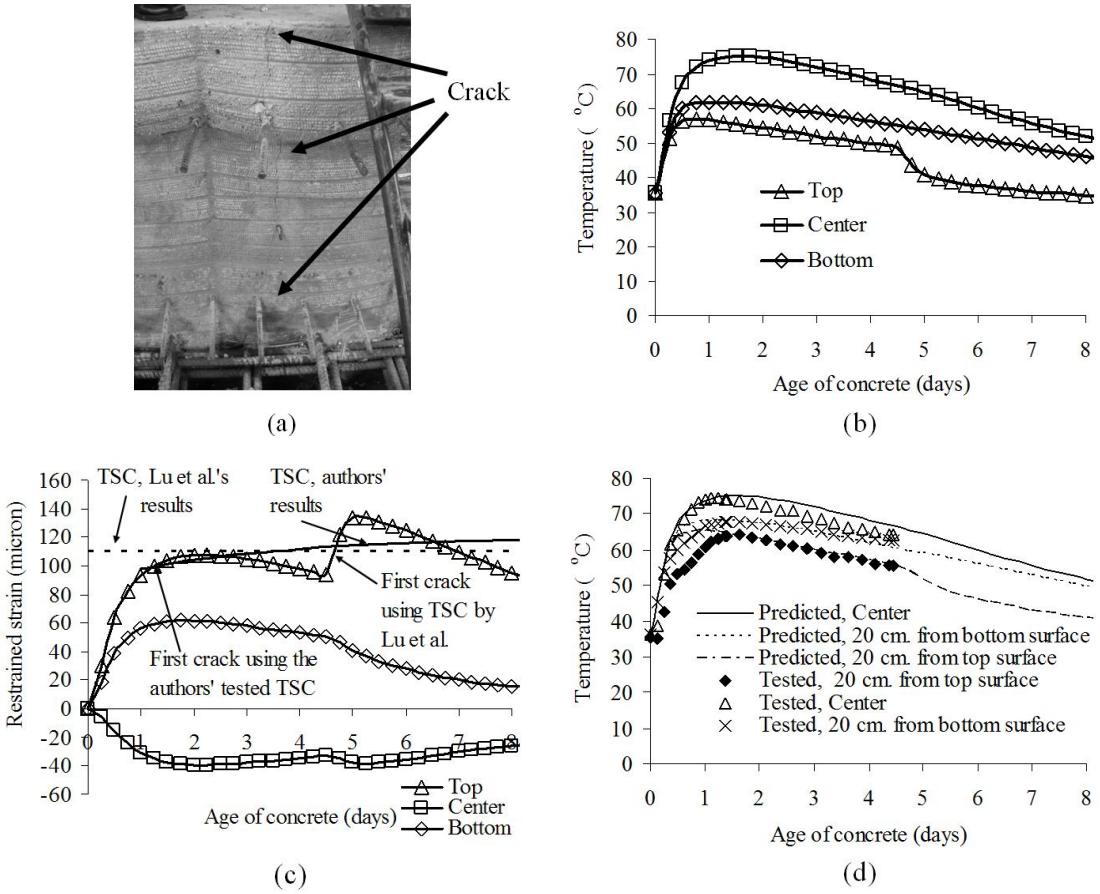

Figure 3. Details of footing no. F4 in Table 2, (a) Crack on side surface, (b) Predicted temperature at top, center and bottom parts, (c) Comparison between tensile strain capacity and predicted restrained strain in lateral direction, (d) Comparison between test and predicted temperature at 20 cm from top surface, center and 20 cm from bottom surface.

The analytical results of temperature and restrained strain at the core zone at top surface, center and bottom surface of the footing are shown in Figures 3b and 3c. The rapid change of temperature and restrained strain after 4.6 days occurs due to the removal of insulation material. In case of temperature, top surface shows the lowest but center shows the highest temperature. For illustration in this paper, temperature at the top surface and the center are used to describe the lowest and the highest temperature, respectively. The different expansion between the center and the surface causes restraint between the center and the surface of the structure. The surface is restrained in tension and the central part is restrained in compression. The analytical results show the same tendency as that occurred in mass concrete as shown in Figure 3c. In this study, the restrained strain is used to explain the phenomena that occur in mass concrete. The restrained strain in tension ($\varepsilon_{res,\,ten}$) at the top surface is the highest then this is used to describe the cracking risk in this study. The $\varepsilon_{res,\,ten}$ at the top surface obtained from the analysis is compared with the authors' tested and other researcher's results of tensile strain capacity of concrete (TSC) and if the $\varepsilon_{res,\,ten}$ is higher than the tensile strain capacity then the mass concrete structure is predicted to crack.

Comparisons between the measured and the predicted temperature at the center, 20 cm from the top and 20 cm from the bottom of the footing are shown in Figure 3d. Verifications showed that the model is satisfactory for predicting temperature of the footing. Figure 3c shows the comparisons between the predicted $\varepsilon_{res,\,ten}$ on the top surface and TSC of the concrete. By comparing the analyzed restrained strain with the authors' test results of TSC, the footing was predicted to crack since early age before the removal of insulation material. Severity becomes higher after the insulation material was removed. The footing was predicted to have first crack after the removal of the insulation material when TSC of concrete proposed by Lu *et al.* (2001) was used in the comparison. Lu *et al.* (2001) stated that when the restrained strain of concrete reaches 111 micron, concrete tends to crack. From the comparison using the authors' proposed model and tested TSC, it can be concluded that the model was satisfactory to predict thermal cracking of the footing.

Hereafter, the above model is used to analyze the effect of thickness, casting method, aggregate type, curing

condition and curing period on temperature and restrained strain of mass concrete.

4. Analytical Parameters

4.1 Mix proportions and properties of concrete

The mix proportions and properties of concrete used in the analysis are shown in Table 3. Mix 1 was used to study the effect of thickness of mass concrete structure, casting method and curing condition. Mixes 1 and 2 were used to investigate the effect of type of aggregate.

4.2 Thicknesses of structure

In order to investigate the effect of thickness of mass concrete, thickness was varied to be 0.5, 1.0, 1.5, 2.0, 2.5, 3.0, 4.0, 5.0, 6.0, 8.0 and 10.0 m. whereas the width and length were fixed at 33 and 49.2 m., respectively. An example of description of the dimension designation is as follow; "d0.5" means the structure which has size 33 x 49.2 x 0.5 m. Insulation curing was used in the analysis.

4.3 Casting methods

Two types of casting methods; continuous casting and discontinuous casting, were used in the analysis. In the case of discontinuous casting method, the mass concrete was divided and cast in many small sizes. Temperature gradient of the mass concrete was minimized by using the technique of layer casting or block casting. In this study, various cases of discontinuous casting were used in the analysis as shown in Figure 4. The dimension of casting blocks are shown in Table 3. Mass concrete was assumed to be cast in 2 parts for both layer casting and block casting (see numbers 1 and 2 in Figures 4a to 4d). The second part was cast 2 weeks after the completion of the first part. The volume of concrete for each part was fixed at 2435.4 m^3. The insulation curing was applied to the top surface for all cases. In order to simulate the most critical situation that will occur at the joints of block casting, the boundary condition at the joint of the first part is modeled to be steel formwork to let the heat at the joints of the first casting of the block dissipate faster. The convective heat transfer coefficient at this joint for the first part is assumed to be equal to 7.5 kcal/m^2 hr °C. The analytical results of concrete block 1 are discussed in the section 5.

4.4 Types of aggregate

Limestone and Quartz were used as coarse aggregates for mixes 1 and 2 in Table 3, respectively. The dimension of 33 x 49.2 x 2.5 m. and insulation curing were used in the analysis.

4.5 Curing conditions and curing periods

Two types of curing; normal curing (NC) and insulation curing, were analyzed. The difference of these two types of curing is on the material which is used to cover the top surface. In the case of NC, the top surface was not insulated while for the insulation curing, the top surface was covered with foam. By the use of insulation material, the surface heat loss at the top surface was controlled then *h* of NC is higher

Table 3. Mix proportions, properties of concrete and ingredients and dimensions of layer and block in different casting methods

Mix proportion and properties of concrete and ingredients		
Mix No.	1	2
Cement (kg/m^3)	212	212
Fly Ash (kg/m^3)	212	212
Water (kg/m^3)	166	166
Coarse Aggregate (kg/m^3)	1120	1120
Fine Aggregate (kg/m^3)	700	700
Type of Coarse Aggregate	Limestone	Quartzite
E at 28 days (MPa)	28000	28000
ν	0.2	0.2
Dimensions of layer and block in different casting methods		
Casting method	Notation	Dimension of layer or block (m.)
Continuous casting	Con	33.0 x 49.2 x 3.0
Discontinuous casting : 2 Layers	2L	33.0 x 49.2 x 1.5
Discontinuous casting : 2 Blocks	2B	33.0 x 24.6 x 3.0
Discontinuous casting : 4 Blocks	4B	33.0 x 12.3 x 3.0

Remark: E and n are modulus of elasticity and poisson ratio, respectively.

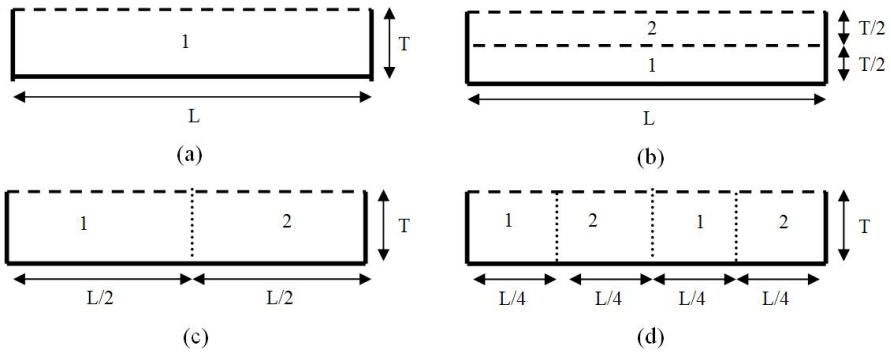

Figure 4. Casting step of mass concrete (side view), (a) Continuous casting, (b). Discontinuous casting with 2-layer casting, (c). Discontinuous casting with 2-block casting, (d) Discontinuous casting with 4-block casting.

than that of the insulation curing. For insulation curing, the curing period were divided into two cases; continuous insulation curing (CIC) and discontinuous insulation curing (DIC). For continuous insulation curing (CIC), the insulation material was kept until the end of the analysis while for the discontinuous insulation curing (DIC), the insulation material was removed a few days after a peak temperature was reached.

5 Analytical Results

5.1 Effect of thickness

Figure 5a shows the prediction of temperature at the center of mass concrete with different thickness. It can be seen that temperature increases with increasing thickness of

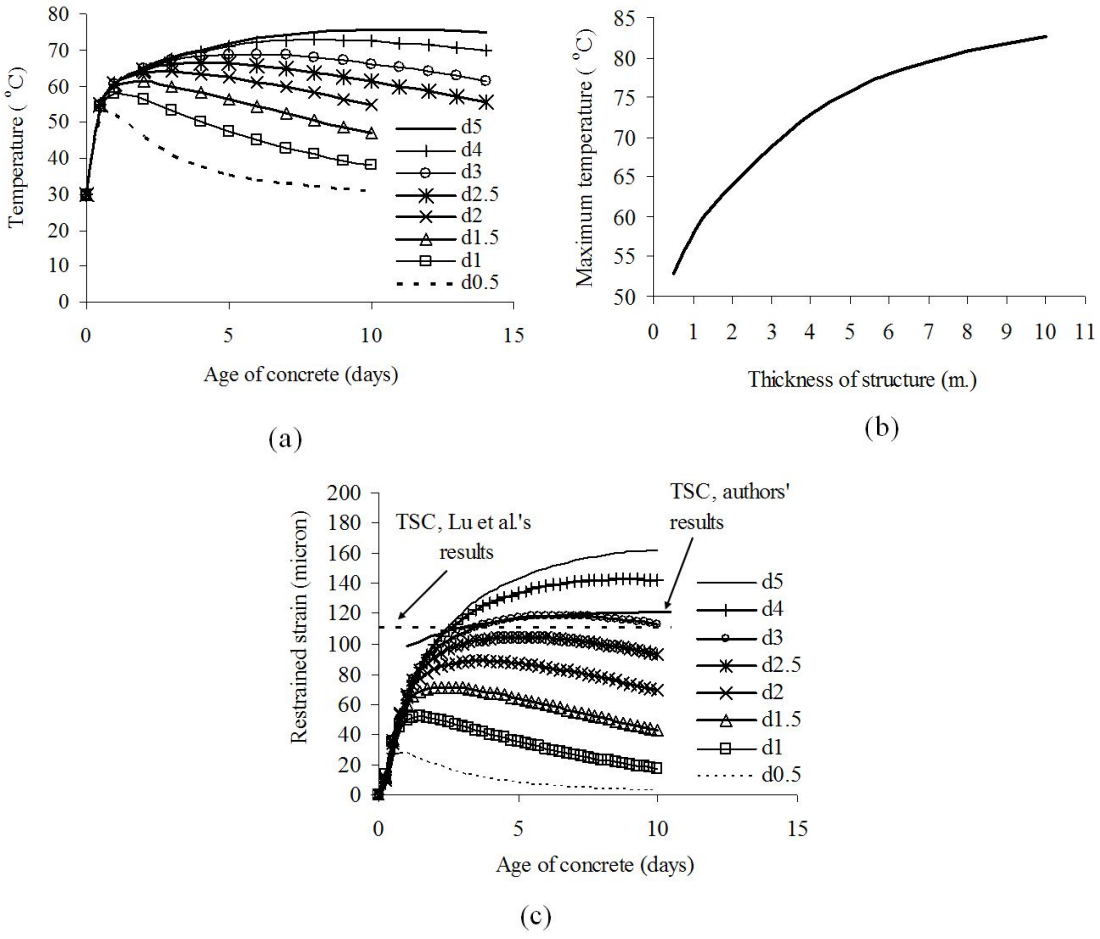

Figure 5. Predicted results of mass concrete with different thickness (width = 33 m., length = 49.2 m), (a) Temperature, (b) Relationship between maximum temperature and thickness, (c) Restrained strain in lateral direction

the mass concrete and the peak temperature age is longer. Figure 5b shows the relationship between the maximum temperature at the center and the thickness of the mass concrete. The maximum temperature increases with increasing thickness. However, when the thickness is thicker, the rate of increase diminishes. When the thickness is large, the behavior of the mass concrete becomes nearly adiabatic. The $\varepsilon_{res,ten}$ (see Figure 5c) shows the same tendency as that of the temperature because temperature difference between the center and the surface is higher when thickness increases.

5.2 Effect of casting method

The analytical results in Figure 5c show that the mass concrete structure with thickness higher than 3 m. tends to crack because the $\varepsilon_{res,ten}$ is higher than TSC. In order to prevent thermal cracking, several techniques are possible. One of them is to apply discontinuous casting method. The footing with the thickness of 3 m. was used as an example to study the effect of casting method.

The analytical results at core zone of concrete block 1, as shown in Figures 6a, 6b and 6c, are used to describe the predicted temperature and $\varepsilon_{res,ten}$ at the top surface in lateral and longitudinal directions of the mass concrete of the first casting part. Figure 6d shows $\varepsilon_{res,ten}$ in the lateral direction of the mass concrete structure at the critical point. From Figure 6a, it can be seen that temperature of different casting methods are nearly the same except for the case of layer casting method. Temperature of concrete is mainly dependent on the thickness (smallest dimension) rather than the width or the length. Thicknesses of the continuous casting and the block casting method are the same but for layered casting the thickness was reduced by half, thence the temperature gradient of the layered casting method is the lowest. From this reason, $\varepsilon_{res,ten}$ of the layered casting method in both lateral and longitudinal direction is the lowest as shown in Figures 6b and 6c. In the case of block casting method, smaller volume of the concrete block results in smaller restrained strain in the lateral direction as shown in Figure 6b (comparing 4B with 2B). The heat loss to the surroundings on the longitudinal surface is highest when compared to other surfaces due to the use of steel formwork. Then temperature gradient between the center and the side surfaces of the block casting method is higher than that in the con-

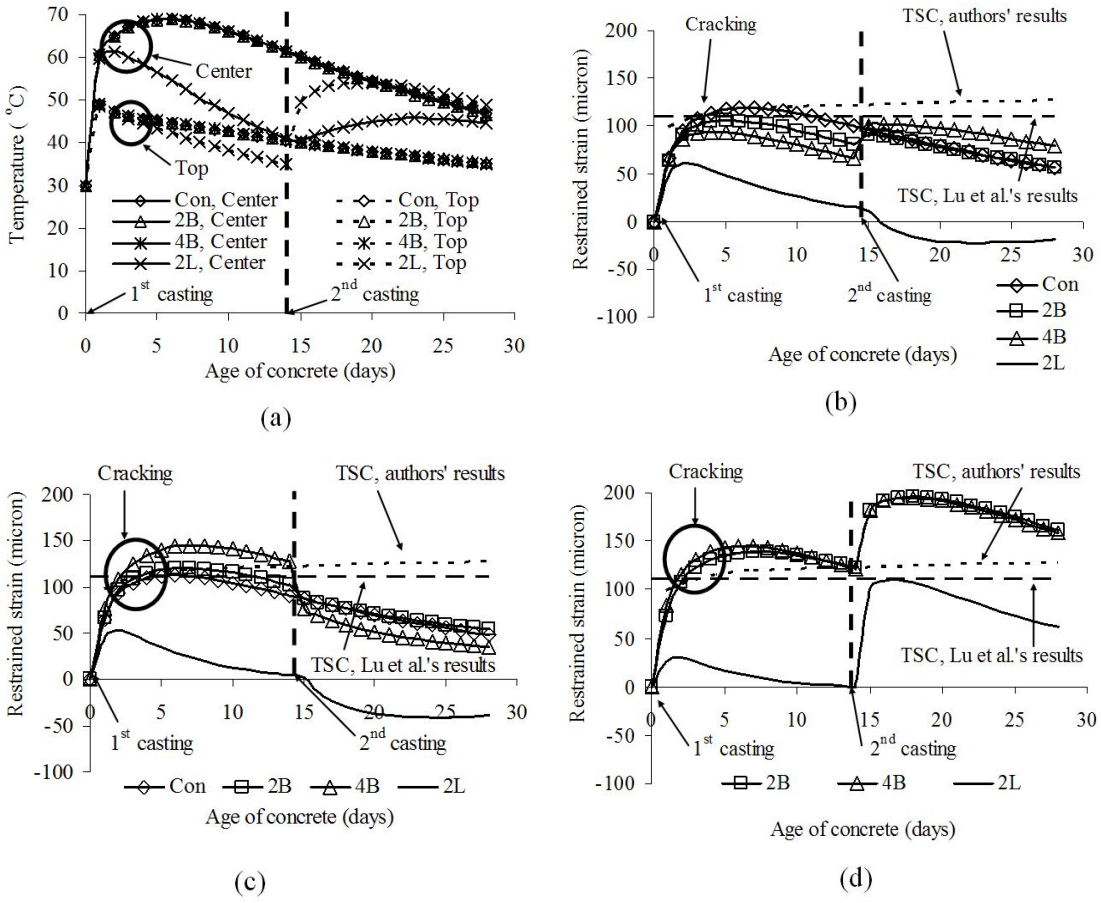

Figure 6. Predicted results of a mass concrete structure with different casting methods, (a) Temperature of the first casting part, (b) Restrained strain in the lateral direction of mass concrete of the first casting part, (c). Restrained strain in the longitudinal direction of mass concrete of the first casting part, (d) Predicted restrained strain in the lateral direction of mass concrete at critical joint.

tinuous casting method. As a result, $\varepsilon_{res,\ ten}$ is higher when compared to the case of continuous casting method (as shown in Figure 6c).

However, the most severe part of block casting occurred at the joint between each block as shown in Figure 6d. According to the use of steel formwork, temperature gradient between the center and this surface is highest when compared to other surfaces thence the $\varepsilon_{res,\ ten}$ on this surface is the highest. When compare $\varepsilon_{res,\ ten}$ to TSC, it was found that both 2B and 4B casting have high chance to crack due to thermal cracking. Figure 6d shows that severity increases after casting of the second block at the cold joint. During heating up stage of the second block, the first block is pulled by the second block, resulting in a rapid increase of restrained strain on the side surface of the first block.

For layered casting, the most critical point occurs at the middle of the bottom surface of the first layer. During heating up stage of the second layer, the heat on the top layer transfer to the bottom layer then the temperature on the top surface of the first layer increases as shown in Figure 6a. This results in the change of phenomena of the footing to be the same as continuous casting where the center is subjected to compressive restraint while the top and the bottom surfaces are subjected to tensile restraint. The $\varepsilon_{res,\ ten}$ at the bottom face increases rapidly after the casting of the second part (as shown in Figure 6d). From Figures 6b, 6c and 6d, $\varepsilon_{res,\ ten}$ was compared to TSC and it was found that layered casting is the most effective method for the control of thermal cracking. In real practice, it is recommended to provide adequate amount of temperature steel near the former cast surface of each cold joint or near the exposed surfaces of the mass concrete in order to reduce the possibility of cracking and to minimize thermal crack widths to be within acceptable values if cracking is unavoidable. It must be mentioned here that in this analysis, the cold joints between each blocks are assumed to have perfect bond. The modulus of elasticity of concrete at an early age, especially at a few hours after casting, is much lower than the value used in this analysis then the increase of the restrained strain after casting of the second block is not as fast as that shown in this paper. However, the analytical results can be used to illustrate the behavior as that occurred in real practices of discontinuous casting of mass concrete with reasonable results.

5.3 Effect of type of aggregate

From Figure 5c, the footing with thickness 2.5 m is safe from thermal cracking when limestone is used as coarse aggregate. However, the use of unsuitable type of aggregate increases crack risk of the structure. Quartzite is used as an example in this study. Figures 7a and 7b show comparisons of temperature and $\varepsilon_{res,\ ten}$ of concrete with different type of coarse aggregates. Quartzite and Limestone have nearly the same specific heat (c) but quartzite has higher thermal conductivity (k) than limestone. As a result, during heating up, temperature of the concrete produced by these aggregates is nearly the same, however during cooling down stage temperature of the quartzite concrete decreases faster than that of the limestone concrete (as shown in Figure 7a). The coefficient of thermal expansion (*CTE*) of quartzite was much higher than that of the limestone thence the restrained strain of the quartzite concrete was much higher than that of the limestone concrete and higher than TSC (see Figure 7b). In this case, the use of quartzite as coarse aggregate causes thermal crack. It can be concluded that for mass concrete limestone is generally more appropriate than quartzite due to much lower *CTE* which reduces restrained strain.

5.4 Effect of curing condition and curing period

As shown in Figure 5c, footing with thickness 2.5 m is safe from thermal cracking when CIC curing method is used. However, the use of inappropriate curing condition and curing period increase crack risk of the footing. Figure 7c shows temperatures at center and top surface of concrete with different curing methods. The temperature difference between the center and the top surface of the structure cured by NC method is higher than CIC method and thence causes higher $\varepsilon_{res,\ ten}$ (as shown in Figure 7d). $\varepsilon_{res,\ ten}$ of NC is higher than TSC thence the use of NC results in higher risk of cracking when compared to CIC. Application of insulation curing is recommended in mass concrete.

Figures 7e and 7f show the temperature and $\varepsilon_{res,\ ten}$ of the concrete footing cured by insulation curing method with varied insulation curing periods. Figure 7e shows that if the insulation material is too early removed (at 7 days), the surface temperature reduces rapidly. As a result, temperature difference between the center and the top surface increases rapidly and thermal cracking may occur. The $\varepsilon_{res,\ ten}$ is higher than TSC when the insulation material is too early removed thence it causes crack after the removal of the insulation material. Figure 7f shows that longer insulation curing period (14 days) results in lower $\varepsilon_{res,\ ten}$. In other words, severity becomes smaller when insulation curing period is longer. As a result, $\varepsilon_{res,\ ten}$ of the longer curing period is always lower than TSC. It is then recommended that temperature monitoring should be conducted to prevent premature removal of the insulation material. The center-ambient temperature difference and the surface-ambient temperature difference at the removal of insulation material should be controlled properly. The insulation curing period should be continued long enough.

6. Conclusion

Based on the analysis of the sample mass concrete using the proposed model, it can be concluded that maximum temperature of the mass concrete increases with increasing thickness of the structure. However, the rate of increase becomes smaller when the structure becomes thicker. The layered casting method is more effective for the control of thermal cracking than the block casting method. Aggregate

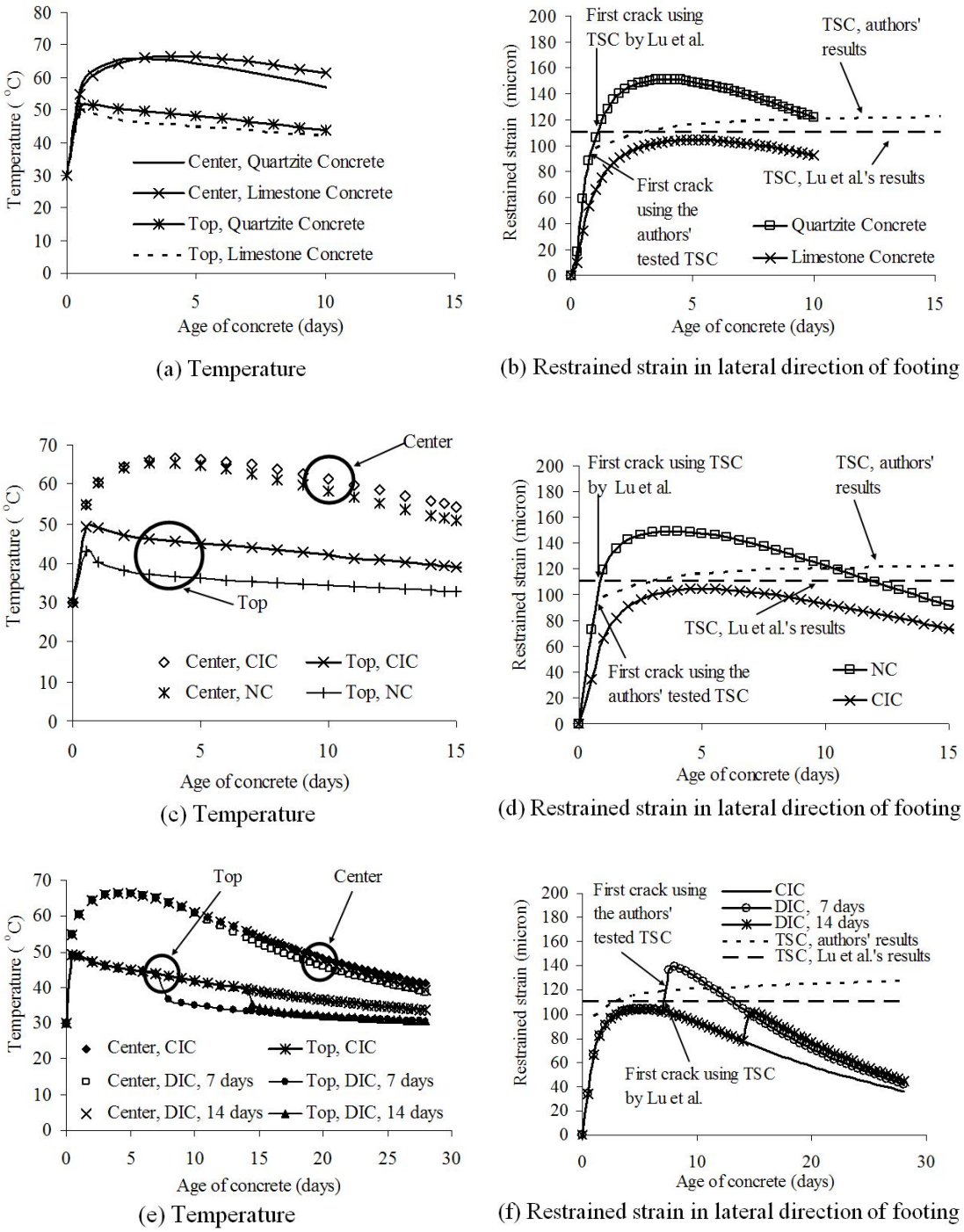

Figure 7. Predicted results of a mass concrete (a) and (b) with limestone and quartzite as coarse aggregates, (c) and (d) cured by normal and insulation curing methods, (e) and (f) cured by continuous and discontinuous insulation curing methods

used in mass concrete should have low *CTE* to lower the restrained strain. The insulation curing method is preferable for mass concrete and in order to prevent cracking, the center-ambient temperature difference and the surface-ambient temperature difference at the removal of insulation material should be controlled properly by providing sufficient insulation curing period.

References

ACI committee 207, 2005, Mass Concrete. ACI manual of concrete practice Part 1. Reported by ACI Committee 207, pp. 207.1R-1 -207.1 R42.

Choktaweekarn, P., Saengsoy, W. and Tangtermsirikul, S. 2009a, A Model for Predicting Specific Heat capacity

of fly-ash concrete, ScienceAsia, 35(2), 178-182.

Choktaweekarn, P., Saengsoy, W. and Tangtermsirikul, S. 2009b. A Model for Predicting Thermal Conductivity of Concrete, Magazine of Concrete Research, 61(4), 271-280

Choketaweekarn, P. and Tangtermsirikul, S. 2006, "Thermal Expansion Coefficient of Concrete", Proceedings of the 10th East Asia Pacific Conference on Structural Engineering and Construction (EASEC-10), Bangkok, Thailand, 3-5 August, 2006, pp. 561-566

Choktaweekarn, P. and Tangtermsirikul, S. 2007. A Study of Dispersion Effect of Fly Ash on Heat of Hydration and Model for Predicting Temperature of Mass Concrete, Proceeding of The Twelve National Convention on Civil Engineering, 2-4 May 2007, Phitsanuloke, pp. 304-309.

Choktaweekarn, P. and Tangtermsirikul, S. 2009. A Model for Predicting Coefficient of Thermal Expansion of Cementitious Paste, ScienceAsia, 35(1), 57-63.

Department of the Army U.S. Army corps of Engineers, 1997, Engineering and Design Thermal Studies of Mass Concrete Structures, Engineer Technical Letter ETL1110-2-542.

Faria, R., Azenha, M. and Figueiras, J.A. 2006. Modeling of concrete at early ages: Application to an externally restrained slab, Cement and Concrete Composites, 28(6), 572-585

Isgor, O.B. and Razaqpur, A.G. 2004. Finite element modeling of coupled heat transfer, moisture transport and carbonation processes in concrete structures, Cement and Concrete Composites, 26(1), 57-73.

Jindawanik, T., Chukiert, K. and Wasuwat, P. 2000. Weather data of Thailand for energy conservation 1981-1998 [CD-ROM]. Thailand: Chulalongkorn University.

Kwak, H.-G., Ha, S.-J. and Kim, J.-K. 2006. Non-structural cracking in RC walls: Part I. Finite element formulation, Cement and Concrete Research, 36(4), 749-760.

Lu, H.R., Swaddiwudhipong, S. and Wee, T.H., 2001. Evaluation of Thermal Crack by a Probabilistic Model using the Tensile Strain Capacity, Magazine of Concrete Research, 53(1), 28 -30.

Maekawa, K., Chaube, R. and Kishi, T. 1999. Modelling of Concrete Performance, E & FN Spon, London

Neville, A. M. 1995. Properties of Concrete. (4th ed.), Longman. London.

Park, K.-B., Jee, N.-Y., Yoon, I.-S. and Lee, H.-S. 2008. Prediction of Temperature Distribution in High-Strength Concrete Using Hydration Model, ACI Materials Journal, 105(2), March-April 2008.

Portland Cement Association, 2003. Design and Control of Concrete Admixtures, 14th ed-CD Version, CD100.1.

Saengsoy, W. and Tangtermsirikul, S. 2003. Model for Predicting Temperature of Mass Concrete. Proceedings of the 1st National Concrete Conference, Engineering Institute of Thailand, Kanchanaburi, pp. 211-218.

Sarker, P.K., Jitvutikrai, P., Tangtermsirikul ,S. and Kishi, T., 1999. Modeling of Temperature Rise in Concrete Using Fly Ash, Concrete Model Code for Asia IABSE Colloquium, Vol. 80, Phuket, Thailand, 1999, pp. 126-132.

Tongaroonsri, S. and Tangtermsirikul, S. 2008. Influence of Mixture Condition and Moisture on Tensile Strain Capacity of Concrete, ScienceAsia, 34(1), 59-68.

Wang, C. and Dilger, W.H. 1994. Prediction of Temperature Distribution in Hardening Concrete, in : Springenschmid R. (Ed.), Thermal Cracking in Concrete at Early Ages, E & FN Spon, London, UK, pp. 21-28.

Whittier, S., Olyniec, J. and Mcglohn, R., 2004. Minimizing Temperature Differentials in Mass Concrete. Concrete International, December 2004, pp. 42-45